Research on Chemical Intermediates
https://doi.org/10.1007/s11164-018-3656-x

Synthesis, characterization and biological activity of mixed ligands complexes of quinolin-8-ol and substituted chromones with Mn(II), Co(II), Ni(II) and Cu(II) metal ions

Nitin H. Kolhe[1] · **Shridhar S. Jadhav**[2]

Received: 1 July 2018 / Accepted: 27 October 2018

Abstract

The mixed ligand complexes were synthesized using quinolin-8-ol and substituted chromone derivative with transition metals like Mn(II), Cu(II), Ni(II) and Co(II). These complexes were characterized using elemental analysis by electron dispersive spectroscopy, Fourier transforms infrared, ultraviolet–visible, proton nuclear magnetic resonance, liquid chromatography coupled with mass spectrometry, electron spin resonance spectra, magnetic susceptibility, powder X-ray diffraction, thermogravimetric analysis and scanning electron microscopy. The complexes were screened by biological activities such as antioxidant activity by 2, 2-Diphenyl-1-picrylhydrazyl, antimicrobial activity by the agar well-diffusion method and anticancer activity by yellow tetrazolium (3-(4, 5-dimethylthiazolyl-2)-2,5-diphenyltetrazolium bromide methods. The synthesis of mixed ligand complexes were synthesized by using homoleptic complexes of respective metal complexes of chromones. The FTIR spectra show ν_{M-O} the ν_{M-N} frequencies are obtained at 515–645 cm^{-1} and 431–496 cm^{-1} respectively. The NMR spectra of Ni(II) complexes were indicating the complexes are paramagnetic in nature. The ESR spectra of copper complexes shows singlet signal, and they indicate that the copper has 2 + oxidation state in complexes. The complexes showed a well-defined crystal system indicated by powder-X-ray diffraction patterns. The thermogram studies show formation of metal oxides residues at the end product of decomposition of complexes. The scanning electron microscope showed complexes were nanocrystalline in nature. The mixed ligand complex of Ni(II) shows 80.73% antioxidant activity as compared to both the ligands and other metal complexes. The antibacterial activity result obtained clearly showed that all complexes were effective against all the microorganisms of *Staphylococcus aures, Bacillus subtilis, Escherichia coli* and *Pseudomonas aeruginos*. The inhibition of the cancerous cell is more the case of Ni (II) complexes as compared with other complexes.

Electronic supplementary material The online version of this article (https://doi.org/10.1007/s11164-018-3656-x) contains supplementary material, which is available to authorized users.

Extended author information available on the last page of the article

Published online: 03 November 2018

Keywords Mixed ligand complexes · XRD · SEM · Antioxidant · Antibacterial · Anticancer

Introduction

The inorganic co-ordinationated chelate complexes play an important role in biology [1]. Most of the organic heterocyclic compounds are biologically active and show activity as anti-HIV [2], antiviral [3], antibacterial [4], anti-inflammatory [5], anti-coagulant [6], and anticancer [7], etc. The good example of an organic heterocyclic compound is chromones [8], and quinolin-8-ol. The mixed ligand metal complexes play an important role in the medicinal field. One of the inorganic anticancer drugs is Cis-DDP [9]. The biological role of transition metal clusters or complexes are important in living organisms such as manganese [10], metal in the Photosystem-II, in a plant body while the Mn-Cluster plays an important role in the human body for the production of dioxygen [11], as well as cobalt in Vitamin B_{12}, and copper in ceruloplasmin. The chromones are also important for biological purposes in plants [12] and for animals in the case of medicinal purposes. The anthocyanidine [13], contains the chromone nucleus which is responsible for the color of the flower. The ligands are biologically active. If we form metal complexes using these ligands then, the activity may be changed. This can be used for the development of new medicine. Thus by using the idea of formation of active complexes we have prepared the inorganic coordination complexes of transition metals like Mn(II), Co(II), Ni(II), Cu(II) with quinolin-8-ol and 6-chloro-4-oxo-4H-chromene-3-carbaldehyde.

Literature surveys show that many chemists have synthesized chromone compound but very few of them worked on the chromones metal complexes [14, 15]. Thus in this paper, we have described the synthesis of ligands and their metal complexes. Further, these were characterized by spectral, thermal, magnetic and some microanalytical methods. The complexes and ligand were tested for their in vitro antioxidant activity by DPPH assay, and antimicrobial activity against the gram positive and gram negative strains using agar well diffusion method [16], the complexes were also screened for anticancer activity.

Experiments

Materials and methods

Metal salts like $NiCl_2{\cdot}6H_2O$, $CuCl_2{\cdot}2H_2O$, $CoCl_2{\cdot}6H_2O$, $MnCl_2{\cdot}5H_2O$ (99.90%, Merck) quinolin-8-ol, $POCl_3$ (99.98%, Merck), dry Pyridine, anhydrous $AlCl_3$ (99.98%, Merck) ethanol, methanol, DMSO, DMF, chloroform and acetic acid (98.99%, Merck) was used as they were for synthesis of ligand and its metal complexes.

A melting point of the synthesized compounds was determined on digital Melting Point/boiling Point apparatus EQ-730 equiptronics and is uncorrected. The IR spectra (KBr Pellets) were measured on an IRAffinity-1 shimadzu FTIR

spectrophotometer in the range 4000–400 cm^{-1}. The electronic spectra for ligands and complexes were recorded on a UV-1800 Shimadzu spectrophotometer in the range 200–800 nm. The electronic spectra of all the complexes were taken at 10^{-3}M concentration in the DMSO and DMF solutions. The magnetic susceptibility was recorded on the Gouy balance method at room temperature by using $Hg[Co(SCN)_4]$ as the calibrate. The molar conductance of complexes was recorded on an Elico conductivity bridge in DMF 10^{-4} M solution using a dip type conductivity cell fitted with a platinum electrode.

The thermal analysis was measured from room temperature to 9500–1000 °C in air and some of the complexes in nitrogen atmosphere heated at non-isothermally with heating rate 8 °C/min. using a TGA-50 Shimadzu thermogravimetric analyser. ^{1}H NMR spectral measurements were performed on a Brucker Acend™ 500 MHz spectrometer. The reported chemical shifts were against TMS, DMSO-d_6 and $CDCl_3$ solvents used for ligands and metal complexes analysis at Department of Chemistry, Savitribai Phule Pune University. ESR spectra were obtained from a JEOL Japan JES FA200 ESR Spectrometer with X-band at room temperature. The ESR spectra were obtained from SAIF, IIT Powai University of Mumbai. Elemental analyses of C, H and N were done on a JEOL C, H, N elemental analyser at the SAIF, Indian Institute of Technology (IIT-Powai), Mumbai University. LC-MS measurements of organic ligand were performed on UHPLC-Ultimate-3000, thermo scientific LC-MS spectrometer at Department of Chemistry, Savitribai Phule Pune University and used for characterization.

Synthesis of ligand

The ligand 6-chloro-4-oxo-4H-chromene-3-carbaldehyde was synthesized by the Vilsmeier-Haack reaction (Scheme 1) by the literature method [17]. The synthesis of 4 chlorophenylacetate **1a** was from 1 mol of 4-chlorophenol by reacting with 1 mol of acetic anhydride in the presence of 5 mL of dry pyridine by the literature method [18].

The obtained product was then run for the Fries reaction by a reported method to form **1b** [19]. The Fries reaction product was further used for the synthesis of 6-chloro-4-oxo-4H-chromene-3-carbaldehyde. In **1b** was obtained 25 mL of dimethylformamide and then 15 mL $POCl_3$ was added drop wise by maintaining the temperature below 20 °C. The whole reaction mixture was stirred with a magnetic stirrer for about 1 h to get a pink formulating complex [20]. The reaction mixture was stirred for a few h and then the reaction mixture was kept at room temperature for overnight. Then the reaction mixture was poured into crushed ice with vigorous stirring. The product was precipitated as a brown solid of 6-chloro-4-oxo-4H-chromene-3-carbaldehyde **1c**, which was filtered and recrystallized from acetic acid.

Synthesis of the complexes of 6-chloro-4oxo-4H-chromene-3-carbaldehyde

The detailed synthesis procedure and synthetic route for homoleptic complexes are shown in Scheme 2.

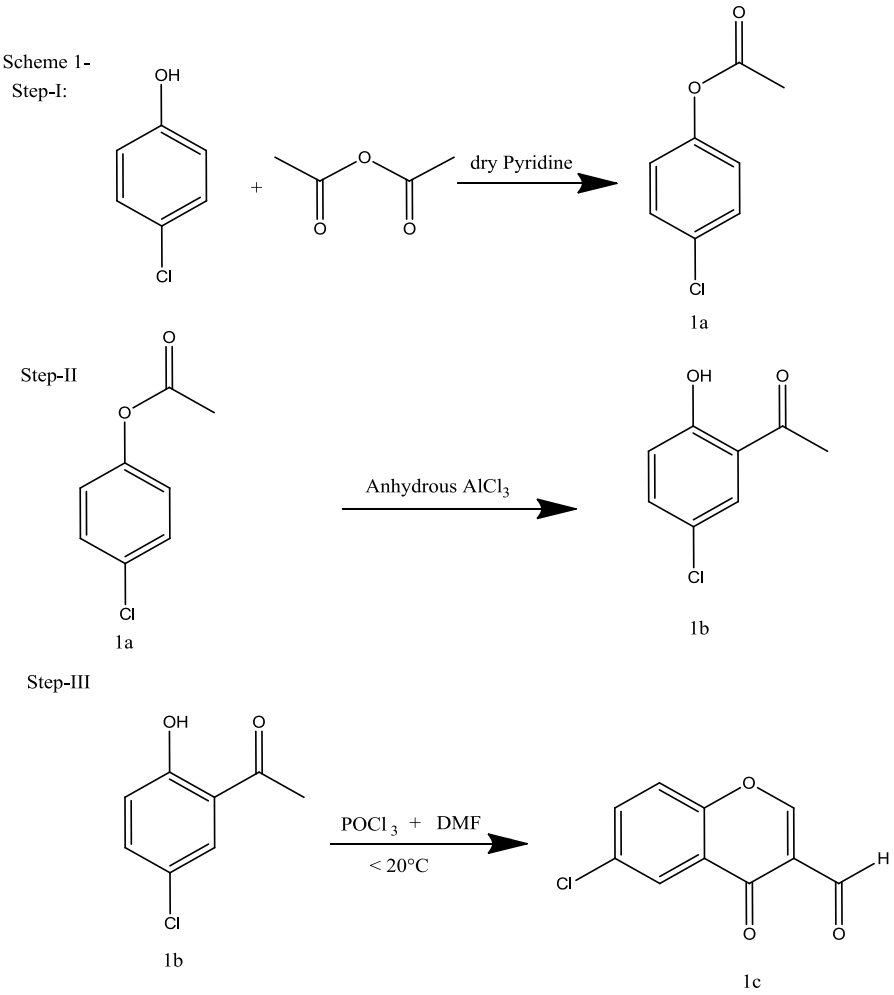

Scheme 1 Synthesis of ligand

Ni(II) complex $[C_{20}H_{10}C_{l4}NiO_6]$ 1

The complex **1** was synthesized by adding a methanolic solution of nickel chloride hexahydrated (0.237 g, 1 mol) to a hot methanolic (10 mL) solution of 6-chloro-4-oxo-4H-chmene-3-carbaldehyde (0.416 g, 2 mol) with vigorous stirring. Then this solution was refluxed at 80–90 °C for 6.5 h. After 6.5 h the solution changes its colour to red solution then 2–3 drops of aqueous ammonia was added and the solution was kept at room temperature for overnight, after which the orange coloured solid was filtered and was air dried. The weight of product was 0.427 g, yield 78.20%.

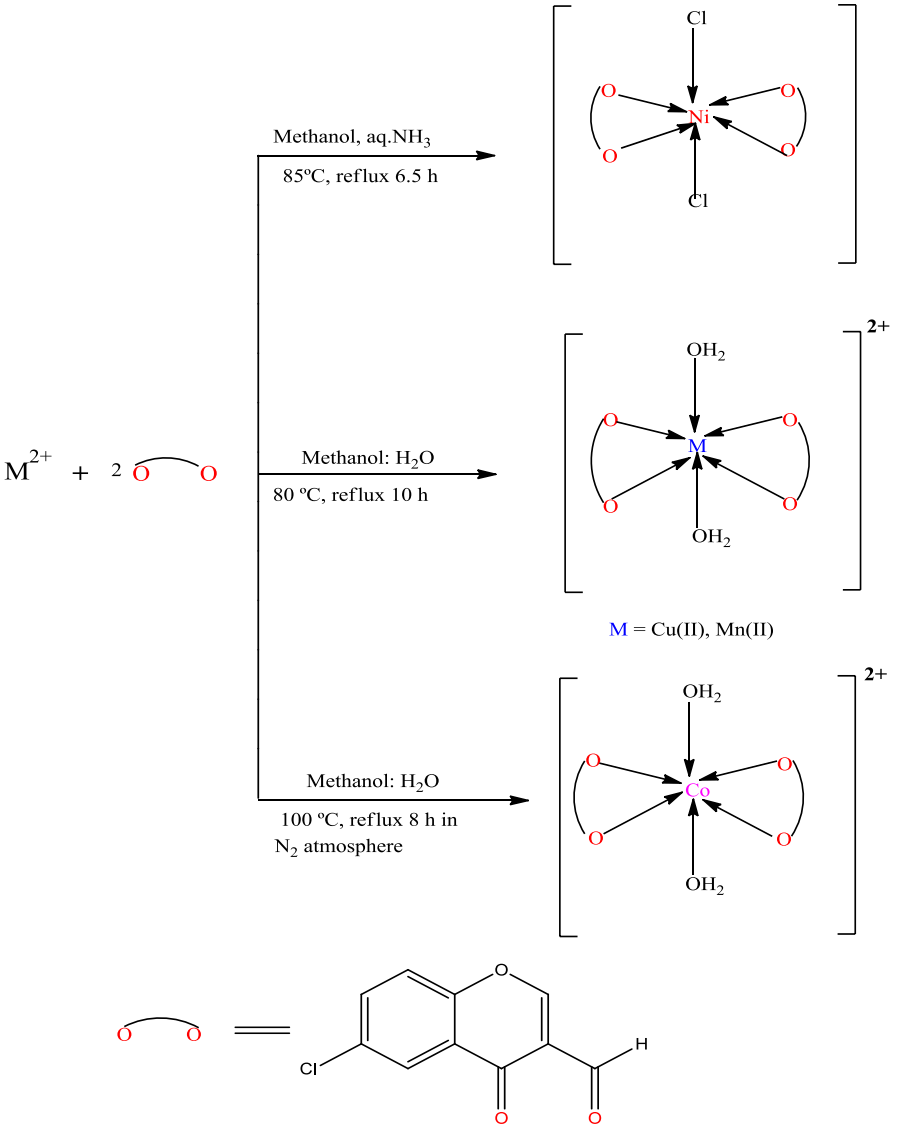

Scheme 2 Synthetic route for homoleptic complexes

Cu(II) complex $[C_{20}H_{14}Cl_2CuO_8]$ Cl_2 2 The copper complex **2** was synthesized by adding ligand (0.416 g, 2 mmol) to hot methanol and adding the Cu(II) salt a solution (0.170 g, 1 mmol in 10 mL methanol) into ligand solution drop wise with constant stirring for 10 min. Then the whole mixture was refluxed for 3 h at 70–80 °C. The little amount of ammonia was added to get a green color solution which was kept for overnight to form the dark green colour complex. The complex was filtered

through a Buchner funnel, washed with methanol and dried at atmospheric condition. The practical yield of a complex is 0.438 g, yield 75.85%.

Co(II) complex $[C_{20}H_{14}Cl_2CoO_8]\ Cl_2$ 3

The complex $C_{20}H_{14}Cl_2CoO_8]\ Cl_2$ was synthesized by reacting the mixture of $CoCl_2{\cdot}6H_2O$ (0.237 g, 1 mmol) and 6-chloro-4oxo-4H-chomone-3-carbaldehyde (0.416 g, 2 mmol) in hot methanol under N_2 atmosphere and refluxed for 8 h, during which brown product was precipitated. Most of the solvent was evaporated and then the product was collected, washed with methanol: H_2O and dried. The weight of product was 0.390 g, yield 67.24%.

Mn(II) complexes $[C_{20}H_{14}Cl_2MnO_8]Cl_2$ 4

The (0.0416 g 2 mmol) 6-chloro-4-oxo-4H-chromene-3-carbaldehyde ligand was dissolved in hot methanol. To this hot ligand solution 10 mL methanolic solution of 0.197 g (1 mol) of Mn(II), the salt solution was added drop by drop with continuous stirring while the temperature was maintained at 80–90 °C for 30 min. Then the whole mixture was refluxed for 12 h and this solution was kept for overnight. Then the 2–4 drops of cold water solution were added to maintain the pH. The complex was a precipitate showing brown colour, which was filtered and washed with methanol. The complex was dried at room temperature. The practical weight of the product was 0.421 g, yield: 72.71%.

Synthesis of mixed ligand complexes of quinolin-8-ol and 6-chloro-4-oxo-4H-chromene-3-carbaldehyde with Ni (II), Cu (II) and Co (II) metal ions

The synthetic route for mixed ligand complexes (Scheme 3) and its preparation is described as follows.

Ni(II) complex $[C_{29}H_{16}Cl_2NNiO_7]Cl$ 5

The complex was synthesized by refluxing the complex **1** (0.271 g, 1 mmol and quinolin-8-ol (0.0725 g, 1 mmol) in hot methanol for 12 h during which the reaction color changes from orange to green. The reaction mixture was evaporated and dried. The product was purified by column chromatography. The practical yield was 0.229 g, % yield 70.67%.

Cu(II) complex $[C_{29}H_{16}Cl_2CuNO_7]Cl$ 6

The complex was synthesized by refluxing the anhydrous complex **2** (0.275 g, 1 mmol) and quinolin-8-ol (0.0725 g, 1 mmol) in hot methanol: acetic acid (1:1, v/v) for 12 h during which green product was precipitated. The solvent was evaporated

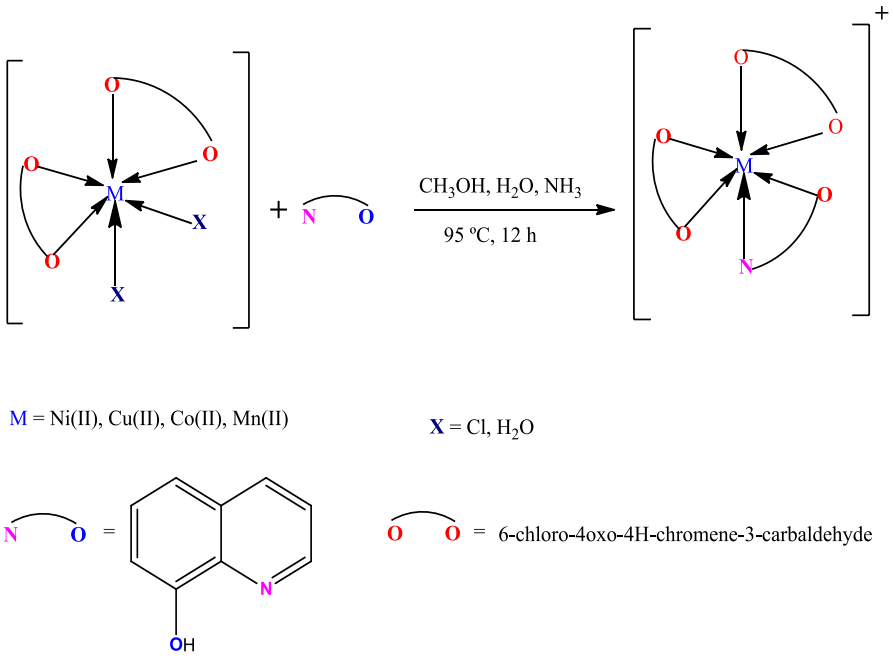

Scheme 3 Synthetic route for mixed ligand complexes

and solid was separated. The product was purified by washing with methanol and dried. The practical yield was 0.251 g, yield 76.29%.

Co (II) complex $[C_{29}H_{16}Cl_2CoNO_7]Cl$ 7

The complex was synthesized by refluxing the dehydrated complex **3** (0.271 g, 1 mmol) and quinolin-8-ol (0.0725 g, 1 mmol) in hot methanol under N_2 atmosphere for 12 h, during which chocolate brown coloured product was precipitated. The solvent was evaporated to dryness, and then the product was filtered, washed with methanol and dried in vacuum. The practical weight of the complex was 0.243 g, yield 75.00%.

Mn(II) complex $[C_{29}H_{16}Cl_2MnNO_7]$ Cl 8

The complex was synthesized by refluxing the dehydrated complex **4** (0.271 g, which was dissolved in hot methanol solution with 1 mL acetic acid and quinolin-8-ol (0.072 g, 1 mmol) in methanol, then the mixture was refluxed for 6 h then the pH was maintained by adding ammonia ammonium chloride buffer during which a brown coloured solution was formed. The solvent was evaporated up to a minimum amount of the solvent remaining and keep for some time until the product appeared. Then the product was washed with methanol and dried in vacuum. The practical yield was 0.216 g, yield 66.46%.

Antioxidant activity

The antioxidant activities of all synthesized complexes were measured by DPPH assay. The synthesized complexes were dissolved in DMSO with different concentrations, that is, 20 mg, 40 mg, 60 mg, 80 mg and 100 mg/10 mL. In each concentration solution 3 mL of methanolic DPPH solution was added. After 30 min, the absorbance of the test complexes and ligand was measured at 517 nm using a UV–Vis spectrophotometer [21]. The standard drug used was ascorbic acid. Free radical antioxidant activity of DPPH is estimated using the formula,

$$\%\text{DPPH inhibition} = \text{Ab}_{\text{control}} - \text{Ab}_{\text{sample}}/\text{Ab}_{\text{control}} \times 100,$$

where, $\text{Ab}_{\text{control}}$ is the absorbance of DPPH radical + DMSO and $\text{Ab}_{\text{sample}}$ is the absorbance of DPPH radical + sample/standard.

Antimicrobial activity

For this study, the test cultures of bacterial strains *Escherichia Coli, Salmonella typhi, Bacillus subtilis* and *Staphylococcus aureus* were maintained in nutrient agar slants at 37 °C. The antimicrobial activity of compounds against test bacteria was determined by the agar well diffusion method [22]. The plates containing 20 mL of nutrient agar were spread with 100 µL of seeded culture. The wells were made on these plates with the help of a borer of 9 mm diameter. The test compounds were loaded (100 µL) into the well as the test sample and DMSO as negative control. The bacterial plates were incubated in an incubator at 37 °C for 24 h. Growth was evaluated visually by comparing a particular plate with the standard antibiotic ciprofloxacin.

Anticancer activity by MTT assay

The cytotoxicity was evaluated by MTT [3-4, 5-dimethylthiazol-2-yl)-2,5-diphenyl tetrazolium bromide) according to Mossmann et al. [23]. Hela cell cultures (5×10^5 cell/ml) were cultured in 96-well flat bottomed microtitreplates and incubated for 48 h. at 37 °C in a humidified 5% CO_2 incubator. Different concentrations of 25, 50, 75, 100 µL of the synthesized complexes were added to the wells. The plate was incubated for 48 h. at 37 °C in a humidified incubator with 5% CO_2. MTT (5 mg/ml) was prepared in phosphate buffer saline (PBS). MTT (10 µl) was added to each well and incubated in the dark for 4 h. in CO_2 incubator. The supernatant was removed from the well and the plate was washed three times with Dulbecco's formula PBS (pH 7.3). DMSO (100 µl) was added to each well. The absorbance of the sample was measured at 570 nm after 30 min. The results of all complexes were compared with standard drug Doxorubicin (10 µM).

Results and discussion

Elemental analysis by electron dispersive X-ray spectroscopy

Elemental analysis of all complexes was analysed by an EDS/EDX spectrum. This shows the stoichiometry of complexes matched with the percentage of C, N, and O. The metal, chloride analysis was also done by EDS spectra; therefore, this was the great advantage of EDS over C, H, N, O analysis of inorganic coordination complexes.

The colour, molecular weight, melting point, elemental analysis and conductivity measurements are illustrated in Table 1 and the EDS spectrum is shown in Supplementary material Fig. S1. The EDS spectral result match with the calculated % of C, O, N, Cl, and particular metals depends on the complexes, so it indicates the formation of complexes. The molar conductance measurements of all the metal complexes **2–8** were found to be electrolytic in nature except for the complex **1.**

Infrared spectra

The most important characteristic frequencies of complexes are shown in Table 2. The assignments were made by comparison of IR bands of free ligand with its metal complexes. The IR spectra of both the two ligands behave as bidentate ligands. The chromone is the O, O donor and neutral ligand, while the quinolin-8-ol is the N, O donor and is mononegative ligand.

The complexes **1**–**4** show the broadband at 3307–3465 cm^{-1} is due to ν_{H2O} and the complexes **5**–**8** show the band is absent because we have used dehydrated complexes for their preparation of mixed ligand-metal complexes. The characteristic band of aldhydic carbonyl was found to be 1710 cm^{-1} in the **L2**. These frequencies lower by the unit 20–139 cm^{-1} in the complexes, indicating that the aldehydes carbonyls donate the pair of electrons toward the metal and forming metal–oxygen bond [24]. The ν_{M-O} frequencies are obtained in the complexes at the 515–645 cm^{-1} and depend on the metal complexes [25]. In the case of the mixed ligand complexes **5**–**8** the ν_{M-N} frequencies are obtained at 431–496 cm^{-1}. The **L1** donate the electron from the C = N atom toward the metal in the case of mixed ligand complexes, in L1 it shows 1540 cm^{-1} and in the complexes it is lower down by 36 cm^{-1} and it clearly indicates a formation bond between ligand and metal in complexes [26].

Electronic spectra of complex and magnetic moments

The electronic spectra (Supplementary material Fig. S2) for the complexes were scan from 200 to 800 nm on the UV–Vis spectrophotometer. The concentration of complexes was in pure DMSO (10^{-3} M). The ultraviolet absorption spectrum of the **L1** shows two bands at positions of 275.15 nm and 314.18 nm, and **L2** shows bands at 282.22 nm and 352.73 nm assigned to $\pi \rightarrow \pi^*$ and $n \rightarrow \pi^*$respectively.

Table 1 Physical and micro-analytical data for ligands and their transition metal complexes

Sr.nos.	Complexes	Color	Mol. wt.	M.P (°C)	Element analysis found (calculated)						Λm ohm^{-1} cm^2 mol^{-1}
					C	H	O	N	Cl	M	
L1	$[C_9H_7NO]$	White	145.15	72–74 °C	74.47(74.50)	4.86(4.86)	11.02(11.00)	9.65(9.58)	–	–	–
L2	$C_{10}H_5ClO_3$	Yellow	208.59	168–169 °C	57.58(57.48)	2.42(2.42)	23.01(22.12)	–	–	–	–
1	$[C_{20}H_{10}Cl_4NiO_6]$	Orange	546.79	112-115d*	43.52 (43.93)	1.82 (1.84)	17.54 (17.56)	–	25.84 (25.94)	10.90 (10.73)	09.83
2	$[C_{20}H_{14}Cl_2CuO_8]$ Cl_2	Dark Green	587.67	169–170d*	40.63 (40.88)	2.38 (2.40)	21.89 (21.78)	–	24.11 (24.13)	10.60 (10.81)	115
3	$[C_{20}H_{14}Cl_2CoO_8]$ Cl_2	Brown	583.06	> 300d*	40.98 (41.20)	2.40 (2.42)	21.56 (21.95)	–	24.30 (24.32)	10.19 (10.11)	138
4	$[C_{20}H_{14}Cl_2MnO_8]$ Cl_2	Brown	579.07	107–110d*	41.28 (41.48)	2.42 (2.44)	22.18 (22.10)	–	23.18 (24.49)	9.46 (9.49)	105
5	$[C_{29}H_{16}Cl_2NNiO_7]$ Cl	Green	655.49	134d*	53.12 (53.14)	2.45 (2.46)	17.18 (17.09)	2.33 (2.14)	16.34 (16.23)	8.88 (8.95)	79.30
6	$[C_{29}H_{16}Cl_2CuNO_7]$ Cl	Faint Green	660.34	107–112d*	52.69 (52.75)	2.30 (2.44)	16.96 (16.99)	2.19 (2.12)	16.33 (16.11)	10.56 (9.62)	78.52
7	$C_{29}H_{16}Cl_2CoNO_7]$ Cl	Brown	655.73	> 300d*	53.08 (53.12)	2.44 (2.46)	17.38 (17.08)	2.08 (2.14)	16.28 (16.22)	8.28 (8.99)	72.63
8	$C_{29}H_{16}Cl_2MnNO_7]$ Cl	Brown	651.73	> 300d*	53.37 (53.44)	2.42 (2.47)	17.14 (17.18)	2.41 (2.15)	16.36 (16.32)	8.65 (8.43)	78.17

*d** Decomposition temperature, *Λm* molar conductance, *L1 Quinolin-8-ol, L2 6-chloro-4-oxo-4H-chromone*

Table 2 The characteristic FTIR band of ligands and their metal-complexes

Sr. nos.	Complexes	υ_{O-H}/H_2O	υ_{C-H}	$\upsilon_{C=O}$	$\upsilon_{C=N}$	υ_{C-O}	υ_{M-N}	υ_{M-O}
L1	$[C_9H_7NO]$	3213	3074	–	1540	1500	–	–
L2	$C_{10}H_5ClO_3$	–	2974	1695	–	1425	–	–
1	$[C_{20}H_{10}Cl_4NiO_6]$	3307	2869	1612	–	1222	–	515
2	$[C_{20}H_{14}Cl_2CuO_8]Cl_2$	3427	2981	1631	–	1222	–	635
3	$[C_{20}H_{14}Cl_2CoO_8]\ Cl_2$	3465	3200	1612	–	1222	–	505
4	$[C_{20}H_{14}Cl_2MnO_8]Cl_2$	3372	3009	1631	–	1250	–	607
5	$[C_{29}H_{16}C2l_2NNiO_7]\ Cl$	–	2819	1690	1504	1261	431	648
6	$[C_{29}H_{16}Cl_2CuNO_7]Cl$	–	2810	1643	1569	1102	496	579
7	$C_{29}H_{16}Cl_2CoNO_7]Cl$	–	2698	1571	1615	1270	430	533
8	$C_{29}H_{16}Cl_2MnNO_7]Cl$	–	2816	1625	1552	1140	421	645

Absorption spectrum of complexes **1** displays three bands at 264 nm, 308.24 nm and 361 nm, respectively, that corresponds to the $^3A_2g\ (F) \rightarrow {}^3T_2g(F)$, $^3A_2g(F) \rightarrow {}^3T_1g(F)$, and $^3A_2g(F) \rightarrow {}^3T_1g(P)$ transitions, which are referred to an octahedral geometry around Ni(II) ion. The mixed ligand complex of nickel complex **5** exhibits peaks at 28,409.09 cm^{-1}, 33,670.03 cm^{-1} and 36,363.04 cm^{-1} attributed $^6A_1g \rightarrow {}^4Eg\ (^4D)$, $^6A_1g \rightarrow {}^4T_2g\ (^4G)$ to, respectively, and suggests octahedral geometry. The magnetic moment value of complex **5** is found to be 3.24 BM, suggesting octahedral geometry.

Magnetic momentum value of the Cu(II) complex **6** is 2.10 BM, and complex **2**, 2.06 falls within the range observed for octahedral geometry. Further, the electronic spectra of Cu(II) complex shows peaks at 27,139.25 cm^{-1}, 28,762.08 cm^{-1}, 32,062.59 cm^{-1} due to transition between $^2Eg \rightarrow {}^2T_2g$ indicating octahedral geometry [27] and the colour of the complex is due to d-d transition. Co(II) complexes **3** and **7** show bands at 32,825.63 cm^{-1}, 37,740.12 cm^{-1}, 43,425.40 cm^{-1} and 14,450 cm^{-1}, 19,011 cm^{-1}, 22,323 cm^{-1} band, respectively, due to the transitions $^4T_1g(F) \rightarrow {}^4T_2g(F)$, $^4T_1g(F) \rightarrow {}^4A_2g(F)$,$^4T_1g(F) \rightarrow {}^4T_1g(P)$ and magnetic moment 5.10BM to 4.95BM suggesting octahedral geometry. The mixed ligand Mn(II) complex **8** shows three absorption peaks at 14,868 cm^{-1} expected for $^6A_1g \rightarrow {}^4T_1g(S)$, at 18,830 cm^{-1} corresponding to $^6A_1g \rightarrow {}^4T_2g(G)$ and a broad band at 21,518–22,688 cm^{-1} that may be due to $^6A_1g \rightarrow {}^4A_1g$, suggesting octahedral geometry. Further, the octahedral geometry is proposed based on the magnetic moment. The magnetic moment of the complex is found to be 5.81 BM, and falls within the range expected for octahedral geometry. While the complex **4** shows two bands at 18,975.33 cm^{-1} and 23,640.64 cm^{-1} and is due to the d-d transitions.

^{1}H NMR spectra of ligand and complex

^{1}H NMR Spectra of ligand show six indications. The chemical shift (δ) was found to be 10.37(s), 8.55(s), 8.28(s), 7.70(dd), 7.52(dd), and 2.51(s) and from this data the ligand was found and it was pure. The PMR of ligand **L2** (Supplementary material Fig. S3) and the complex are shown in Fig. 1.

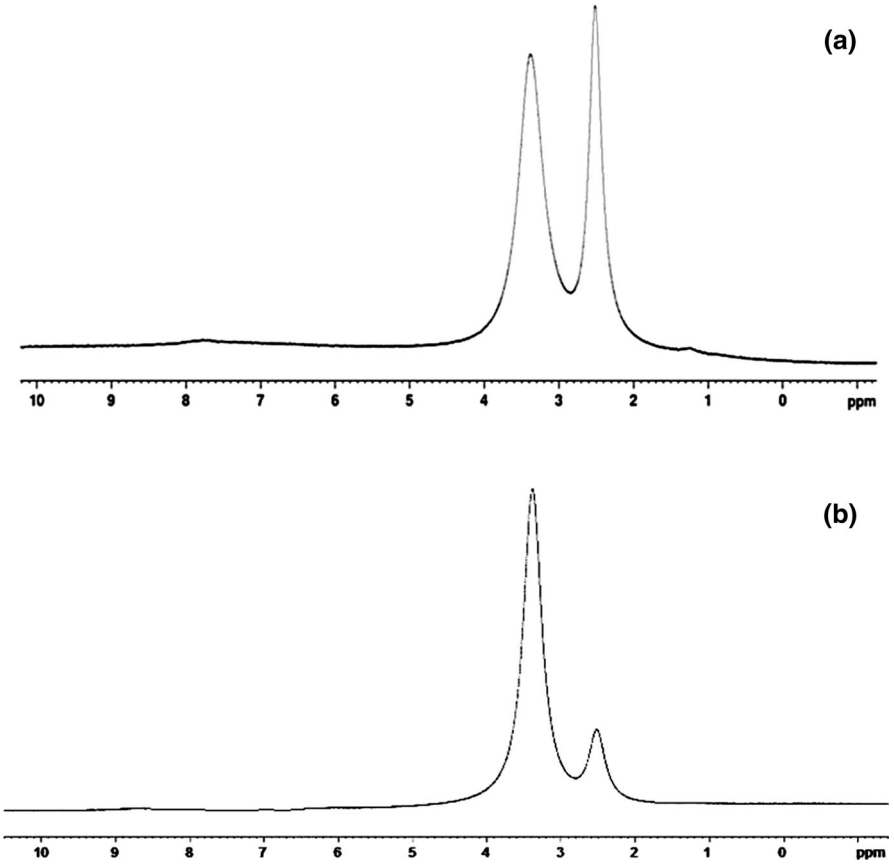

Fig. 1 NMR spectrum of Ni(II) mixed ligand metal complex **1** (**a**) and complex **5** (**b**)

Complex **1** spectrum Fig. 1a and for complex **5** spectrum Fig. 1b show broad spectra indicating the Ni(II) complexes are paramagnetic in nature. The peak obtained for complex **5** δ at 3.3.89 (s) and δ at 2.521 are broad singlets so these are paramagnetic in nature. The aldehydic proton peak was not seen in spectra therefore it donates the electron toward the metal and formation of complexes. Similarly for complex **1** shows two signal δs at 3.383 and a second signal δ at 2.516. Both the peaks were broad it, and they indicate that there was formation of a complex and the complex was paramagnetic in nature.

LC-MS spectra of ligand (L2)

Mass spectrum of ligand **L2** shows a molecular ion peak [M + H] at m/z 208.88, which corresponds to its chemical formula. The LC-MS spectrum of ligand is shown in Supplementary material Fig. S4.

ESR spectra of Cu(II) complexes 2 and 6

ESR spectra of Cu(II) complexes **2** and **6** (Fig. 2) was recorded at room temperature in the polycrystalline state, on X-band at frequency of 9107.60 MH_Z under the magnetic field strength of 298.303 mT. The spectrum of complex **2** shows one intense absorption in the high field and is isotropic due to tumbling of the molecule.

The g values of the complex are of g value 2.322 which is more than the free ion g value (2.0023) indicating that the unpaired electron in the ground state of Cu(II) that is in $dx^2 - y^2$. While the ESR spectrum of complex **6** shows superhyperfine lines. The signal shows the triplet is due to the Cu nucleus coupled with the nitrogen of the ligand quinolin-8-ol and gives a triplet intense line. So that it indicates that only one molecule of the quinolin-8-ol binds to the copper metal and forms a Cu–N bond. It also indicates that the unpaired electron delocalised through the structures [28].

X-ray diffraction study

The powder XRD pattern (Supplementary material Fig. S5 (a) and (b) of all the homoleptic and heteroleptic complexes were recorded over the $2\theta = 20°–80°$ range. The all metal complexes including mixed ligand complexes exhibit a crystalline nature with sharp peaks. This XRD study is also one of the pieces of evidence about formation of metal-ligand complexes. The XRD unit cell parameter such as crystal nature, bravis lattices, diffraction angles, cell length, volume, etc., are illustrated in Table 3. The XRD peak at the bottom side is broad in all the complexes to indicate smaller particle size may be in nanometers.

Average size of these complexes was calculated by Scherer's formula [29].

$$D = \frac{0.94\lambda}{\beta \cos\theta}$$

where λ is wavelength of X-ray radiation, β is the full width at half maximum of diffraction line and θ is the diffraction angle.

The average crystallite sizes of all the complexes were found to be in nanometer scale. Therefore, we have taken the SEM pictograph. The XRD pattern gives the information about the crystal system and the complexes shows a different crystal nature with different bravis lattices.

Thermogravimetric analysis of complexes

Thermogravimetric studies (TG) for the complexes were carried out from room temperature to 1000 °C. The stages of decomposition, temperature range, and decomposition products as well as the observed mass loss percentages of all complexes are studied. The thermogram of all the complexes is shown in Fig. 3(a) and (b).

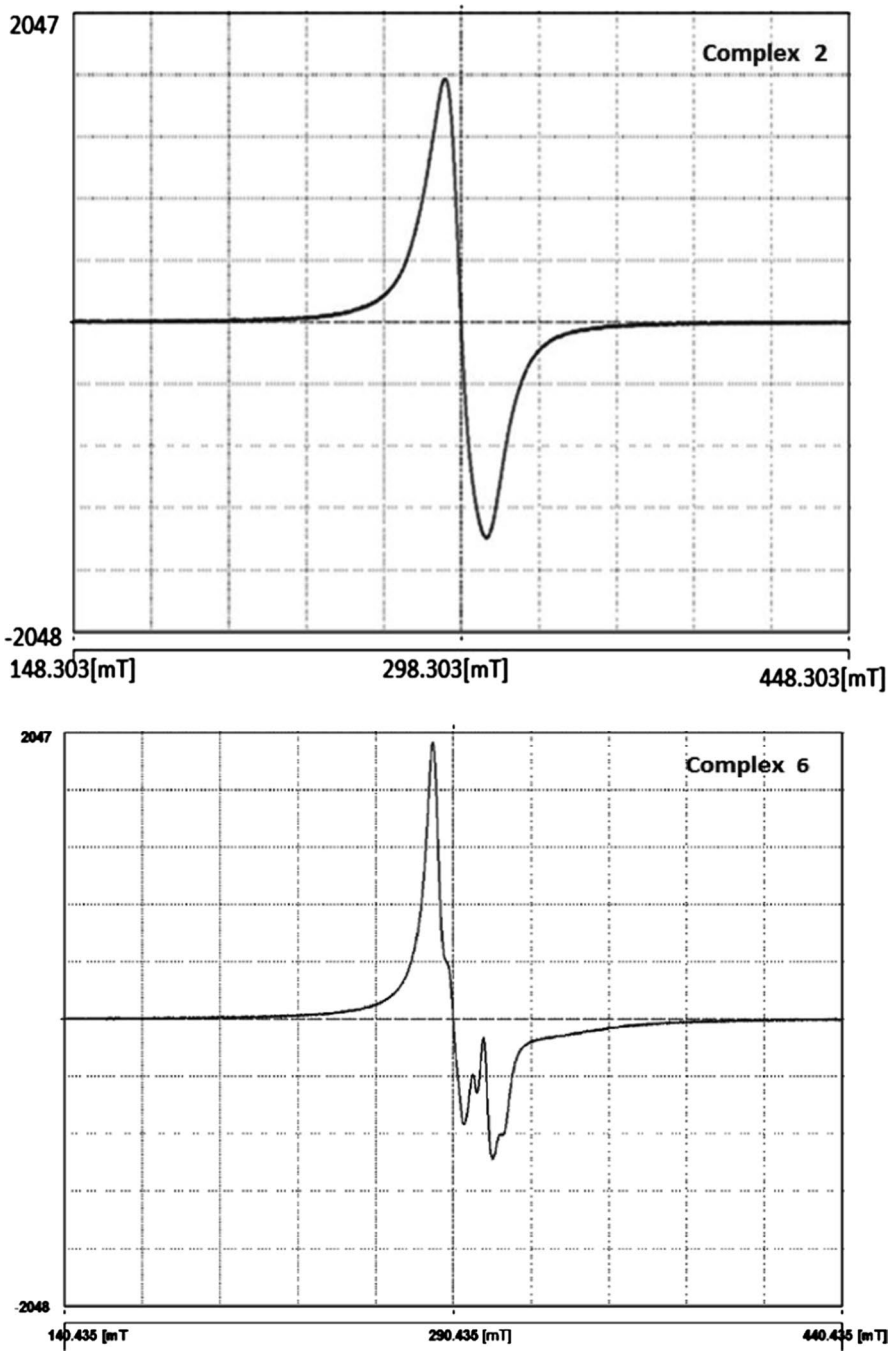

Fig. 2 ESR Spectra of Cu(II) complexes **2** and **6**

Table 3 Powder diffraction parameters of the complexes **1–8**

Complexes	1	2	3	4	5	6	7	8
JCPDS.NO.	48–2466	25–0901	25–1625	48–2399	42–1925	73–1343	28–1590	30–1784
Formula weight	546.79	587.67	583.06	579.07	655.49	660.34	655.73	651.73
Crystal color	Orange	Dark Green	Brown	Brown	Green	Green	Chocolate Brown	Brown
Temperature (K)	298	298	298	298	298	298	298	298
Wavelength (Å)	1.54051	1.54051	1.540598	1.540598	1.54050	1.54051	1.540598	1.540598
Radiation	Cu Kα	Cu Kα	Cu Kα	Cu Kα	Cu Kα	Cu Kα	Cu Kα	Cu Kα
Crystal system	Orthorhombic (I)	Monoclinic (P)	Monoclinic (I)	Tetragonal (P)	Triclinic	Orthorhombic	Monoclinic (I)	Triclinic
a (Å)	14.50	8.44	7.91	15.18	8.88	13.063 (2)	13.185 (7)	16.9644
b (Å)	17.72	11.77	7.06	15.18	8.52	9.9017 (18)	17.546 (8)	5.8213
c (Å)	18.38	4.77	10.07	13.43	7.50	17.472 (3)	6.871 (3)	4.9345
α (°)	90	90	90.00	90	99.93	90	90.00	102.655
β (°)	90	93	101.3	90	116.72	90	107.01	95.222
γ (°)	90	90	90	90	90.02	90	120.00	101.200
a/b	0.7449	0.7757	1.4263	0.7255	0.7449	0.7757	0.7388	0.7255
c/b	0.5245	0.6056	1.1204	0.5235	0.5245	0.6056	0.3916	0.5235
Volume (Å3)	562	474.11	551.45	656	562	3549.47	1520.03	656
Dx **(g/cm)^3**	1.591	1.509	1.87	1.42	1.891	1.509	1.738	1.77

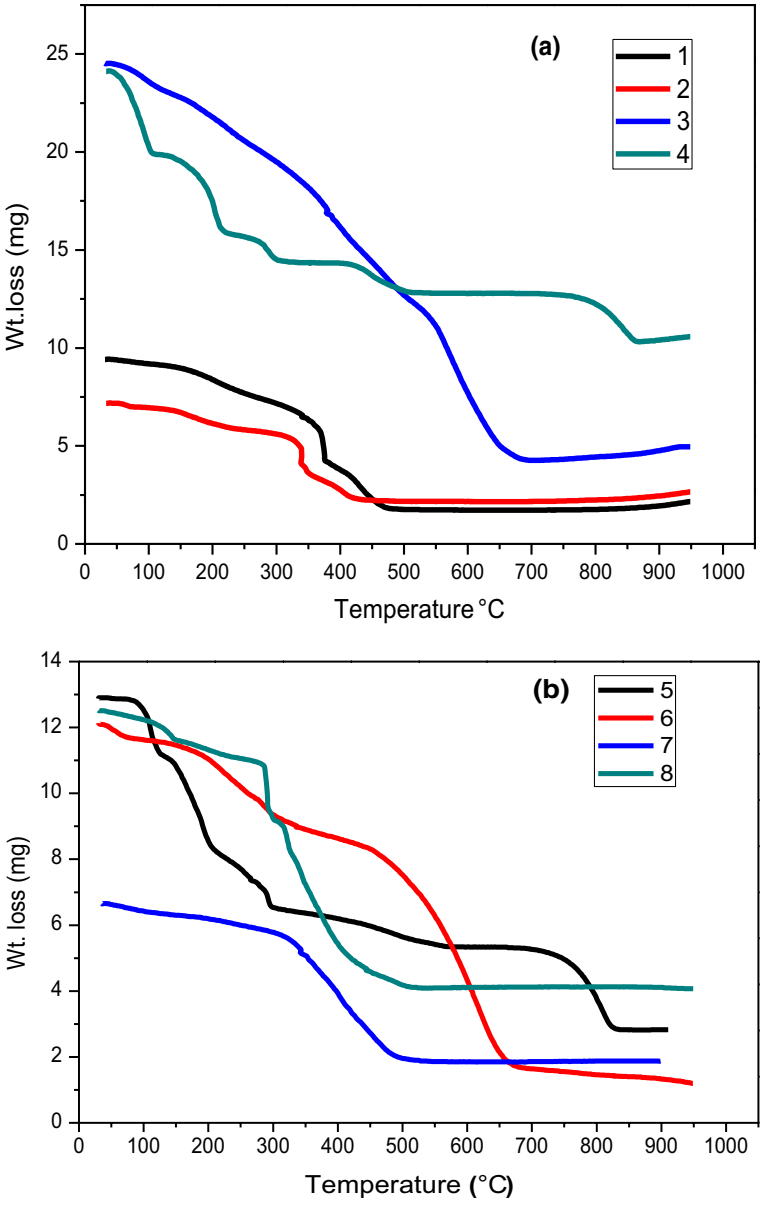

Fig. 3 Thermogram of complexes **1**–**4** (**a**) and **5**–**8** (**b**)

The TG of complex **1** shows single step decomposition between the temperatures 356–382.70 °C with % wt. loss 82.78%, which indicate that organic moiety and chloride ions are evaporated and the remaining NiO as a product was formed.

The complex **2** decomposes into two steps. In the first step for the $H_4Cl_2O_2$ group there was the loss at temperature 255 °C and in the second step the $C_{10}H_5ClO_3$ there

was the loss at temperature 480.67 °C leaving the CuO as residue [30]. The complex **3** shows one step decomposition in the thermogram. In these steps both the coordinated water molecules and chromones were lost between the temperatures 150–643.82, and the % wt. loss was found to 83.61%; this is a match with calculated % wt. loss and finally the formation of cobalt oxide as a product. The thermograph of Mn(II) complex **4** of a homoleptic complex showed the vertical curve at temperatures 272–342 °C with loss of an organic part of the complexes and formation of black residue of MnO_2. Complex **5** showed total % weight loss was found to be 84.582% that matches with calculated wt. loss for 85.64% at temperatures 175–650 °C. The complex **5** was decomposed at temperatures 366–568 °C with loss of both the ligands.

The mixed ligand complexes **6–8** are more stable as compared with their homoleptic complexes. The decomposition occurs in one step. The first step was due to the loss of the ligands chromone and quinolin-8-ol simultaneously and remaining is the metal oxide residue that depends on the metal complexes. All data of the complexes were imputed into Table 4.

Scanning electron microscopy

The surface morphology and the grain size of the metal complexes have been illustrated by the scanning electron micrograph. The SEM micrograph of all the metal complexes is shown in Fig. 4.

Table 4 Thermogravimetric analysis of complexes

Sr. no.	Complexes	Temperature (°C)	% Weight loss found (calculated)	Decomposition assignment
1	$[C_{20}H_{10}Cl_4NiO_6]$	200–382	82.00 (80.00)	$–C_{20}H_{10}Cl_4O_6$
		382–650	18.00 (20.00)	NiO
2	$[C_{20}H_{14}Cl_2CuO_8]Cl_2$	57.37–255	22.16 (23.49)	$–H_4Cl_2O_4$
		300–689	43.27 (45.01)	$–C_{10}H_5ClO_3$
				CuO
3	$[C_{20}H_{14}Cl_2CoO_8]\ Cl_2$	209–643	82.179 (83.61)	$–C_{20}H_{14}Cl_4O_8$
			18.12 (16.97)	Co_3O_4
4	$[C_{20}H_{14}Cl_2MnO_8]Cl_2$	272–342.15	89.69 (89.25)	$-C_{20}H_{14}Cl_4O_8$
			10.12 (11.54)	MnO_2
5	$[C_{29}H_{16}Cl_2NNiO_7]\ Cl$	366–568	83.52 (85.64)	$–C_{29}H_{16}Cl_2NO_7$
			16.50 (14.66)	NiO
6	$[C_{29}H_{16}Cl_2CuNO_7]Cl$	527.10–650.41	84.95 (85.64)	$–C_{29}H_{16}Cl_2NO_7$
			15.05 (14.35)	CuO
7	$C_{29}H_{16}Cl_2CoNO_7]Cl$	150–443	80.46 (83.85)	$–C_{29}H_{16}Cl_2NO_7$
		545–669.47	19.33 (16.15)	CoO
8	$[C_{29}H_{16}Cl_2NNiO_7]\ Cl$	388.50–570	69.46 (70.77)	$–C_{29}H_{16}Cl_2NO_7$
			30.20 (25.78)	MnO_2

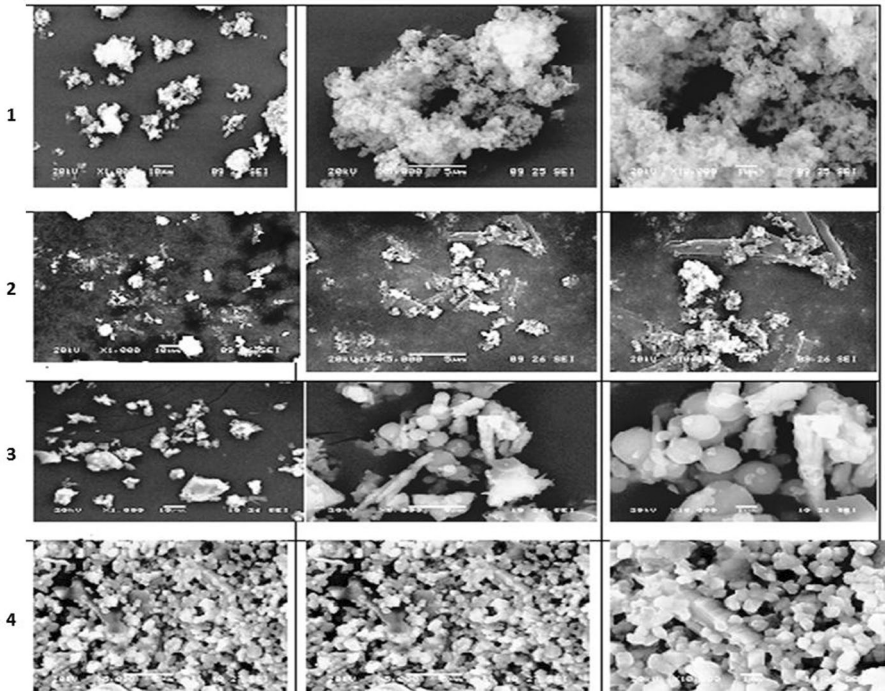

Fig. 4 SEM micrographs of all metal complexes

The complex **1** shows stone shape nanoparticles with the presence of a well in the stone, while the complex **2** does not give fine nanoparticles. The complexes **3** and **4** show spherical shape and aggumlation type shape. The formation of the metal complex has the reduction of phase separation and softness of the surface [31]. The SEM image shows that there was a change in the morphology of complexes to mixed ligand metal complexes [32].

SEM micrograph taken in the three different scales 5 µm, 10 µm, 20 µm. From the SEM analysis all complexes have been shown to be nanocrystalline in nature. The mixed ligand complexes **5**–**8** shows pod, rough rock, spherical ball and the flower type shapes, respectively and the nanocrystalline sizes are 10.15, 8.80, 9.27, 13.45 nm. While for the complexes **1**–**4** the grain size was found to be deep well, rock, ball, and stone like morphology, respectively, and the sizes for complexes are 8.52, 5.87, 5.07, 7.67 nm with the different morphology obtained for the different complexes. It also clearly indicates that the morphology was also changing to changes for the homoleptic complexes that are changes into the heteroleptic complexes.

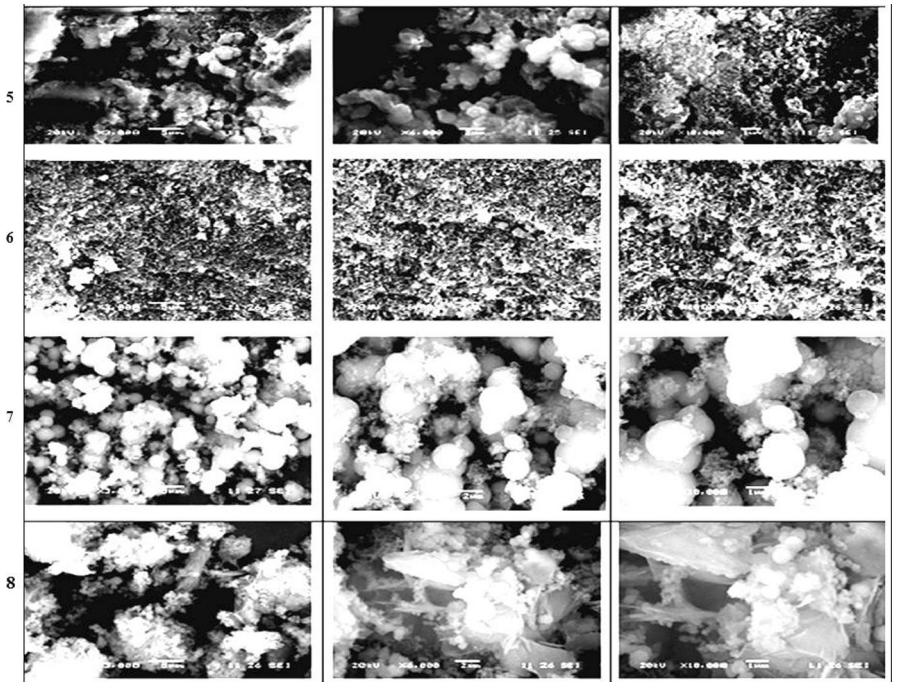

Fig. 4 (continued)

Biological activity

The biological activity of ligand and their metal complexes were screened for antioxidant activity by DPPH assay, antibacterial activity and anticancer activity by MTT assay methods.

Antioxidant activity

Free radicals are generated by enzymatic and non-enzymatic processes and if the colours of these free radicals disappear, it is understood that the compounds have the ability to scavenge free radicals [33].The antioxidant activity of ligand and synthesized complexes have been evaluated for DPPH radical scavenging assay against the ascorbic acid that was used as a reference drug at various concentrations. The percentage of scavenging activity and the IC_{50} value are elaborated in Table 5 and the graph was plotted % S.A. versus concentration (mg) in Fig. 5(a) and (b).

The mixed ligand complex **5** of Ni(II) shows 80.73% scavenging activity as compared to both the ligands and other metal complexes. While these Ni(II) complexes show IC_{50} at 40.60 mg. The complexes of Cu(II) show 48.27 percent scavenging activity and the IC_{50} value is more at 103. 93 mg. The complex of cobalt shows % S.A. 66. 62% and IC_{50} was 57.12 mg, Mn(II) complex shows % S.A. 45.62% and

Table 5 Percent scavenging activity and inhibition concentration of ligands and their metal complexes

Comp.	% S.A.	IC_{50} (mg/mL)
L1	31.45	164.88
L2	77.91	50.45
1	78.57	43.27
2	34.44	251.76
3	65.50	57.67
4	45.77	119.78
5	80.73	40.61
6	48.27	103.93
7	66.62	57.12
8	45.62	109.04
Ascorbic acid	71.77	36.10

IC_{50} 109.04 mg. In the case of all these complexes the Ni(II) complex shows very good scavenging activity at the least concentration that is below 50 mg. The **L1** and **L2** show 31.45% and 77.91% scavenging activity as compared with **L1,** the **L2** shows highest % S.A. The chromone has an IC_{50} value that was 50.45 mg and quinolin-8-ol shows 164.88 mg. Thus chromone ligand and Ni(II) complexes showed good antioxidant complexes [34].

Antimicrobial activity

In antimicrobial activity of the ligands 6-chloro-3-formyl chromone, N,O donor and their mixed ligand complexes with Mn(II), Co(II), Ni(II) and Cu(II) complexes against gram positive *S. aureus, B. subtilis* and gram negative bacteria like *E. coli, P. aeruginos* was carried out. Only the mixed ligands synthesized complexes were dissolved in a minimum quantity of DMSO and adjusted to make up the volume to get 100 µg/mL, 200 µg/mL, 300 µg/mL, 400 µg/mL, 500 µg/mL concentrations. The zone of inhibitions was observed and measured to compare with ciprofloxacin as standard drug. The result obtained clearly showed that all complexes were effective against the entire microorganisms of *S. aures, B. subtilis, E. coli, and P. aeruginoswas*. The zone of inhibition was described in Supplementary material Table T1 and Fig. S6. The Complexes **6** and **7** show more activity as compared with complexes **5** and **8**. The antimicrobial activity goes on to increase with increased concentration in all the complexes [35]. Many researchers found that the less active compound become more active upon complexion [36]. This is due to the decrease in polarity by forming a chelate complex [2].

Anticancer activity by MTT assay

The effect of different complexes was checked on the cancerous cell line. The result of the cytotoxicity assay was expressed in terms of percentage inhibition of

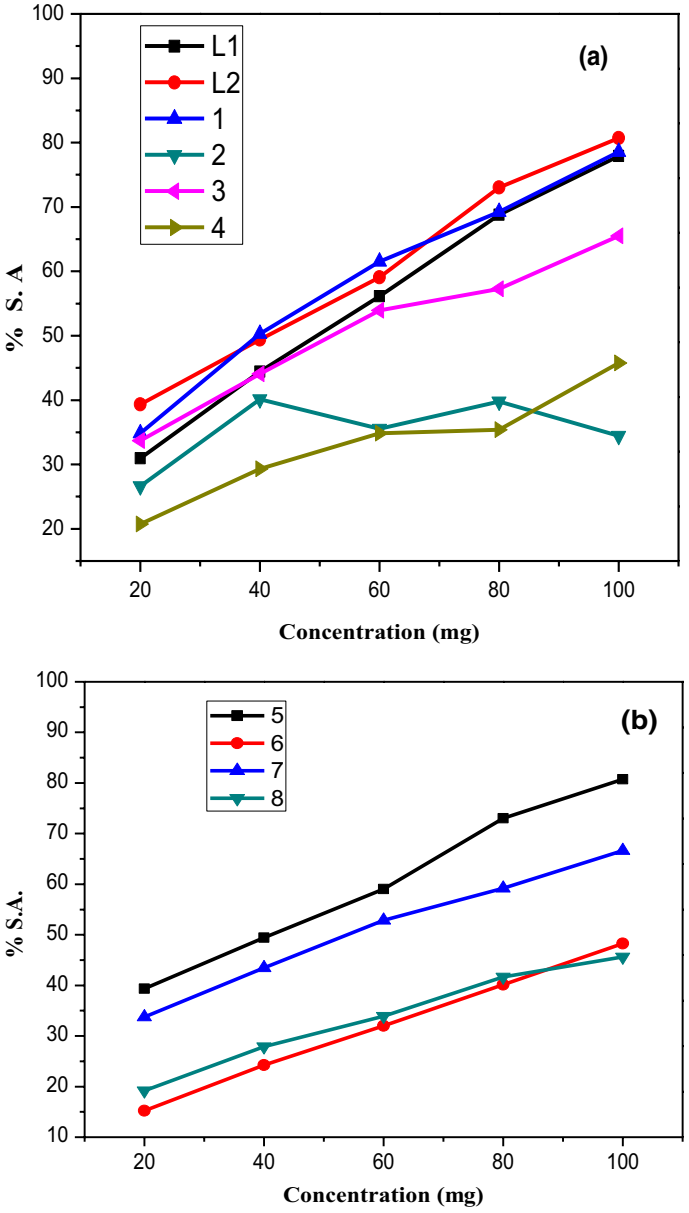

Fig. 5 Antioxidant activity of ligands **L1**, **L2** and complexes **1**–**4** (**a**) and **5**–**8** (**b**)

cancerous cells. The control standard drug Doxorubicin (10 Mm) vial and remaining vials contained chemically synthesized metal–ligand complexes with variable concentration.

The MTT assay was referred to for checking the anticancer activity of the complexes **1**–**8**. The anticancer activity of the complexes was evaluated against the

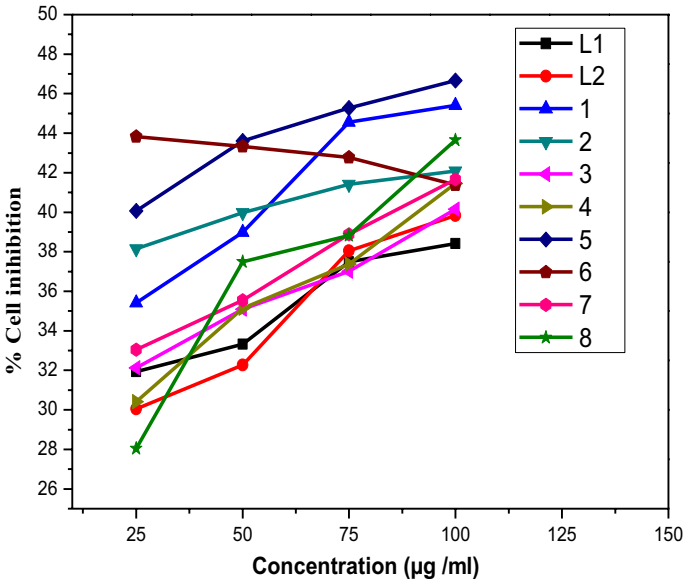

Fig. 6 Anticancer activity of ligands and complexes

Hela-cell line. All the complexes **1**–**8** showed good anticancer activity against the HeLa cell line shown in Fig. 6. Figure 6 was plotted with % cell inhibition versus concentration in µg/mL of complexes. It clearly indicates that the concentration goes on increasing as the % cell inhibition increases. The complexes **1** and **5** showed excellent activity against the other complexes. The complex 5 shows 46.66% cell inhibition at 100 µg/mL. While 1 shows 45.40% inhibition. These complexes also show good activity at lower concentration of 35.42% and 40.06% at 25ug/mL concentration. As followed by complexes **1** and **5** complexes **2** and **6,** these showed 42.08% and 41.38%, respectively, at the highest concentration. The complex **8** shows variable activity with different concentration, at highest concentration the complex **8** showed 43.65% cell inhibition. At lowest concentration, this complex showed very low cell inhibition 28.05%, as compared with **L1**, **L2** and all remaining complexes. The complexes of Co(II) **3**, **7** showed 40.15, 41.66% cell deaths. The Mn(II) complex **4** showed moderate activity, the activity of homoleptic complex **4** showed good with different concentration, but in case of complex **8** it was different. From Fig. 6, this indicates that the concentration increases with increasing anticancer activity in all the complexes except for the complex **8**. Overall complexes like **1**, **5**, **2**, **6**, and **7** show good activity and the other **3**, **4**, **8** displayed moderate activity (Supplementary material Table T2). The result indicates that mixed ligand metal complexes showed good activity as compared with ligands and homoleptic complexes. This is may be due to the change in stereochemistry, structure-relationship activity and induction of activity through the ligand into the metal complexes [37].

Conclusion

We have synthesized heteroleptic complexes from the homoleptic complexes with good yield. Most of the complexes were more biologically active than the ligands molecules. The bonding mode of **L1** was via phenolic oxygen and nitrogen donor atoms, while the **L2** was bound to metals ions through two carbonyl oxygen atoms. The bonding modes of ligand have been elucidated by FTIR, ESR spectra. The geometry of all the chelated complexes were octahedral in nature as was indicated by electronic and magnetic studies. In the case of antioxidant and anticancer activities of the heteroleptic Ni(II) complex; it showed higher activity than the other complexes and the ligands. This has been due to the ligand inducing its activity by forming the chelate complex due to change in its stereochemistry, potential. The antimicrobial activity of complexes was more as compared with ligands, especially heteroleptic complexes that showed higher activity.

Acknowledgements The authors are very grateful to Principal Dr. Muktaja Mathkari, MES, Abasaheb Garware College, Pune and Principal Dr.B.H.Zaware, New Arts Commerce and Science College Ahmednagar for support and providing a laboratory facility. Authors are thankful to HOD, Prof. R.C.Chikate, MES, Abasaheb Garware College Pune for encouragement. Authors are thankful for BCUD, Savitribai Phule Pune University for providing funds under a minor research project (Project No. 14SCI000295).

References

1. N.S. Youssef, K.H. Hegab, A.E. Eid, Synth. React. Inorg. Metal-Org. Chem. **37**, 1647 (2007)
2. Z.H. Chohan, M.S. Iqbal, S.K. Aftab, J. Enz. Inhib. Med. Chem. **47**, 223 (2010)
3. C.M.M. Santos, V.L.M. Silva, A.M.S. Silva, Molecules **22**, 1665 (2017)
4. D.E. Nichols, C.F. Barfknecht, D.B. Rusterholz, F. Benington, R.D. Morin, J. Med. Chem. **16**, 480 (1973)
5. C.M.M. Santos, A.M.S. Silva, A. Lévai, ARKIVOC. **2012**, 265 (2012)
6. L. Lei, Y. Xue, Z. Liu, S. Peng, Y. He, Y. Zhang, R. Fang, Sci. Rep. **5**(1), 1 (2015)
7. D. Hyuk, K. Yong, C. Sang, Y. Sup, Eur. J. Med. Chem. **45**, 4288 (2010)
8. A. Novel, Tetrahedron Lett. **13**, 1183 (1974)
9. E.R. Jamieson, S.J. Lippard, Chem. Rev. **99**, 2467 (1999)
10. D.M. Boghaei, S.J.S. Sabounchei, Synth. React. Inorg. Metal-Org. Chem. **30**(8), 1535 (2000)
11. B. Wang, Z.-Y. Yang, M. Lü, J. Hai, Q. Wang, Z.-N. Chen, J. Organomet. Chem. **694**, 4069 (2009)
12. I. Tinoco, Annu. Rev. Phys. Chem. **53**, 1 (2002)
13. P. Jayaseelan, S. Prasad, S. Vedanayaki, R. Rajavel, Int. J. Pharmac. Res. Synth. **1**, 80 (2010)
14. A. Dziewulska-ku, J. Therm. Anal. Calorim. **101**, 1019 (2010)
15. J. Wiley, Special Trends Therm. Anal. **45**, 1605 (1995)
16. M. Patil, R. Hunoor, K. Gudasi, Eur. J. Med. Chem. **45**, 2981 (2010)
17. Vilsmeier Haack, Aus d. Chem. Laborat. d. Universitat Erlangen **119**(16), 4 (1926)
18. O. Meth-cohn, B. Tarnowski, A. Heterocycl. Chem. **31**, 207 (1982)
19. K. Fries, G. Finck, Chem. Ber. **41**(3), 4271 (1908)
20. G. Jones, S.P. Stanforth, Org. React. **56**(2), 355 (2000)
21. S. Khan, W. Ahmad, K. Munawar, S. Kanwal, Indian J. Pharm. Sci. **80**(3), 480 (2018)
22. S.A. Khan, S. Shahid, W. Ahmad, U. Fatima, S. Knawal, Indian J Pharm Sci. **80**(1), 173 (2018)
23. T. Mosmann, J. Immunol. Methods **65**, 55 (1983)
24. S. Basak, S. Sen, S. Mitra, C. Marschner, W.S. Sheldrick, Struct. Chem. **19**, 115 (2008)
25. K. Rizwan, N. Rasool, R. Rehman, T. Mahmood, K. Ayub, T. Rasheed, G. Ahmad, A. Malik, S.A. Khan, M.N. Akhtar, N.B. Alitheen, M. Nazirul, M. Aziz, Chem. Cent. J. **12**, 84 (2018)

26. M. Aslantaş, E. Kendi, N. Demir, A.E. Şabik, M. Tümer, M. Kertmen, Spectrochim Acta Part A Mol. Biomol. Spectrosc. **74**, 617 (2009)
27. D.P. Singh, R. Kumar, V. Malik, Transit. Metal Chem. **32**, 1051 (2007)
28. D.X. West, D.X. West, A.E. Liberta, Coord. Chem. Rev. **123**, 49 (1993)
29. P. Kavitha, K. Laxma Reddy, Arab. J. Chem. **9**(4), 596 (2016)
30. N. Ahmad, M. Alam, P. Kumar, A. Hashmi, R. Wahab, Asian J. Chem. **25**(18), 10386 (2013)
31. F. Yakuphanoglu, I. Erol, Y. Aydogdu, M. Ahmedzade, Mater. Lett. **57**, 229 (2002)
32. L.A. Saghatforoush, R. Mehdizadeh, F. Chalabian, J. Chem. Pharm. Res. **3**(2), 691 (2011)
33. W. Ahmad, S.A. Khan, K.S. Munawar, Trop. J. Pharm. Res. **16**(5), 1137 (2017)
34. M.A.R. Bhuiyan, M.Z. Hoque, S.J. Hossain, World J. Agric. Sci. **5**(3), 318 (2009)
35. S.A. Khan, S. Shahid, S. Kanwal, G. Husaain, Dye. Pigment. **148**(C), 31 (2017)
36. S.A. Khan, S. Shahid, S. Kanwal, K. Rizwan, T. Mahmood, K. Ayub, J. Mol. Struct. **1175**(C), 73 (2018)
37. G. Hussain, S.A. Khan, F. Noreen, S. Kanwal, A. Iqbal, Mater. Sci. Eng. C **82**(C), 46 (2017)

Affiliations

Nitin H. Kolhe[1] · Shridhar S. Jadhav[2]

✉ Nitin H. Kolhe
kolhenitin18@gmail.com

[1] Department of Chemistry and Research Centre, MES, Abasaheb Garware College, Pune, Affiliated to Savitribai Phule Pune University, Pune 411004, India

[2] Department of Chemistry and Research Centre, New Arts, Commerce and Science College, Ahmednagar 414401, India